International Journal of Mass Spectrometry 300 (2011) 31–38

Contents lists available at ScienceDirect

International Journal of Mass Spectrometry

journal homepage: www.elsevier.com/locate/ijms

Selected ion flow tube (SIFT) studies of the reactions of H_3O^+, NO^+ and $O_2^{+\bullet}$ with six volatile phytogenic esters

Kristýna Sovová [a,b], Kseniya Dryahina [a], Patrik Španěl [a,*]

[a] J. Heyrovský Institute of Physical Chemistry of Science, Academy of Science of the Czech Republic, Dolejškova 3, 18223 Prague 8, Czech Republic
[b] Department of Physical and Macromolecular Chemistry, Faculty of Science, Charles University, Albertov 2030, 12840 Prague 2, Czech Republic

ARTICLE INFO

Article history:
Received 25 October 2010
Received in revised form
29 November 2010
Accepted 30 November 2010
Available online 7 December 2010

Keywords:
SIFT-MS
Ion-molecule reactions
Plant esters
Proton transfer
Charge transfer
Adduct ion formation

ABSTRACT

The selected ion flow tube (SIFT) was used to study the reactions of the three SIFT-MS precursor ions H_3O^+, NO^+ and $O_2^{+\bullet}$ with six phytogenic esters: hexyl acetate, phenethyl acetate, benzyl acetate, methyl salicylate, methyl benzoate and benzyl benzoate. These compounds are emitted into the atmosphere by various species of plants and play a role in communication between individual plants and also amongst different species. Thus, it is necessary to know the rate constants and branching ratios of the different ion products of these reactions for identification and quantification by SIFT-MS. The results of this study show that the reactions of H_3O^+ with the esters proceed via proton transfer, which is non-dissociative for methyl salicylate, entirely dissociative for benzyl benzoate and partly dissociative for the remaining four esters. All protonated esters readily associate with water molecules with the notable exception of methyl salicylate. All six NO^+ reactions result in formation of adduct ions in parallel with charge transfer or with reactions leading to fragment ions. All six $O_2^{+\bullet}$ reactions proceed by charge transfer with the production of one or two major fragment ions; the parent molecular radical cation is formed in three reactions only. Kinetic library entries allowing unambiguous quantification of the six esters by SIFT-MS are presented together with their experimental validation.

1. Introduction

The phytogenic volatile organic compounds (VOCs) are generally small molecules that play an important role in various aspects of plant physiology including growth, development and communication between individual plants and also amongst different species. Some VOCs are released by plants continuously under normal physiological conditions, these include ethylene, isoprene, terpenes, sesquiterpenes [1] methanol [2] and some esters including benzyl acetate, phenethyl acetate, methyl benzoate and benzyl benzoate [3]. However, plants may respond to damage or externally induced stress by releasing specific types of molecules exemplified by hexyl acetate [4], and methyl salicylate that is known to be released by plants in response to damage caused by herbivores [5] and actually acts as an elicitor of foraging predatory mites [6]. The objective of the present study is to obtain kinetic data on ion molecule reactions of the six esters shown in Scheme I with the three commonly used SIFT-MS precursor (reagent) ions H_3O^+, NO^+ and $O_2^{+\bullet}$.

The ion chemistry of these SIFT-MS precursor ions with these esters has not been previously studied except for methyl salicylate which has been studied by Iachetta et al. [8]. The earliest SIFT studies were concerned with a series of simpler esters [9]. SIFT-MS has been successfully used for measurements of the concentrations of some flavourant biogenic monoterpenes and sesquiterpenes emitted by vegetation such as myrcene, ocimene, α- and β-pinene, α- and γ-terpinene, 2- and 3-carene, *R*- and *S*-limonene and camphene [10,11]. In those studies it was observed that the H_3O^+ reactions with the monoterpenes (M), proceeded via proton transfer and result in formation of the protonated molecules MH^+ at an m/z value of 137 and partly of a fragment ion at an m/z of 81. The NO^+ reactions proceeded via charge transfer resulting mainly in the ionized monoterpenes $C_{10}H_{16}^+$ [10]. Thus, using H_3O^+ and NO^+, SIFT-MS can be used to measure the total collective concentration of these terpenes in air. Their reactions with $O_2^{+\bullet}$ result in greater amount of fragments.

VOC emissions from plants, after extraction, can be very effectively studied using the well proven separation methods of gas and liquid chromatography [12,13]. The main shortcoming of these methods is that they cannot provide real time quantification, which is the main practical advantage of the SIFT-MS method. Proton-transfer reaction mass spectrometry, PTR-MS, which is in some aspects similar to SIFT-MS, is also capable of quantification of VOCs

---

[*] Corresponding author. Tel.: +420 2 6605 2112; fax: +420 2 8658 2307.
E-mail addresses: spanel@seznam.cz, patrik.spanel@jh-inst.cas.cz (P. Španěl).

1387-3806/$ – see front matter © 2010 Elsevier B.V. All rights reserved.
doi:10.1016/j.ijms.2010.11.021

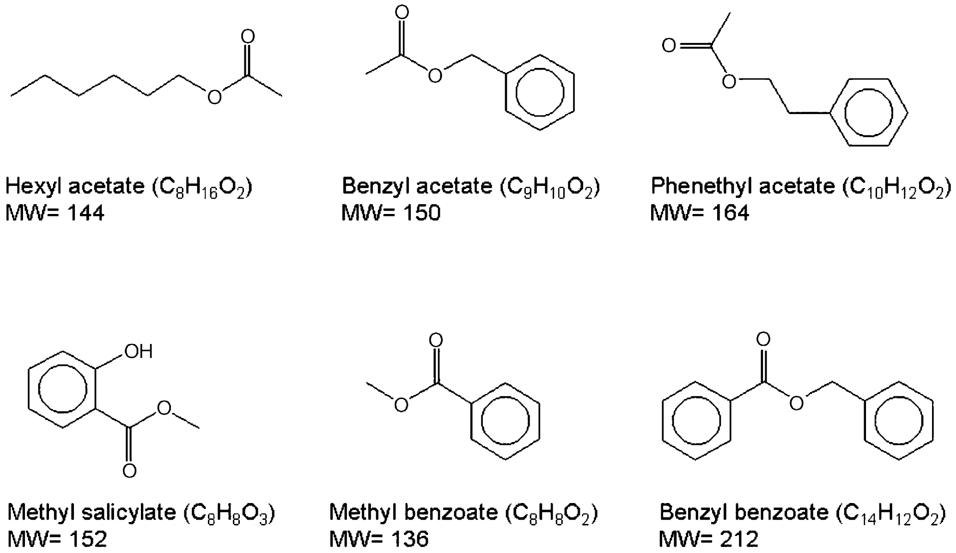

Scheme I. Chemical structures (according to [7]), summary formulas and molecular weights of the six studied phytogenic esters.

in real time [14] and has been used to analyse ethyl and methyl esters in the headspace of water and water/ethanol solutions [15]. PTR-MS has been also used to quantify total collective amounts of mono- and sesquiterpenes both in laboratory studies and in VOC emissions by trees [16,17].

One of the important objectives of the research of VOCs released by plants relates to the capability of various types of plants to clean up contaminated soil and water in the so-called phytoremediation process. One variant of this is phytovolatilization where plants take up contaminants from water or soil and release them into the atmosphere. The question is whether or not the final gaseous products resulting from phytovolatilization cause any secondary pollution of the environment. Thus, the present ion chemistry study involving plant VOCs will facilitate differentiation between the natural (baseline) plant volatiles and the possible additional volatile products resulting from the process of phytovolatilization.

2. Experimental methods

The SIFT technique [18] has been described many times for determination of the rate constants (often called rate coefficients in the field of ion chemistry) and ion product distributions of the reaction of H_3O^+, NO^+ and $O_2^{+\bullet}$ with organic compounds [8–11,18,19]. Thus, only the specific detail of the present experimental procedure, are outlined below.

2.1. *Determination of the branching ratios and the rate constants of ion-molecule reactions*

In order to determine the product ions and their branching ratios, a sample mixture of dry air and a trace amount (typically less than 10 ppm) of vapour of a compound of interest (one of the six esters purchased from Sigma–Aldrich with stated purity of >99%) was introduced into the SIFT instrument (*Profile 3* SIFT-MS manufactured by Instrument Science Limited, Crewe, UK) via a heated calibrated capillary and full scan mass spectra were acquired whilst each of the three selected precursor ions were alternately injected into the helium carrier gas. The *m*/*z* mass spectral range was chosen as 10–250 covering the molecular weights of the six chosen esters and allowing for possible formation of adduct ions. For each precursor ion, five mass spectra were obtained with a total integration time of 60 s. The major ion products were identified and their count rates were precisely determined in separate experiments using the multi-ion monitoring (MIM) mode [18]. In order to determine the primary product branching ratios of the reactions, it is required to plot the percentages of the individual product ions on a linear scale as a function of the sample mixture flow rate determined accordingly to the exponential reduction of the precursor ion count rate (see such a plot for hexyl acetate in Fig. 1). By extrapolating to zero flow (i.e., estimating the limit at zero sample concentration) the true primary branching ratios, excluding any secondary reactions can be obtained. Only product ions with resulting branching ratio greater than 5% are reported.

It is well established that proton transfer reactions of H_3O^+ proceed at the collisional rate as described by the collisional rate coefficient k_c when these reactions are exothermic by more than 40 kJ/mol [20]. Thus, the rate constants for the reactions of H_3O^+ were calculated as collisional (k_c) according to Su and Chesnavich [21] using the dipole moment and polarisability data from [22–25]. The rate constants for the reactions with NO^+ and $O_2^{+\bullet}$ (k) were then derived from their experimentally derived decay rates relatively to that for the H_3O^+ reaction [26] by injecting all three precursors simultaneously and allowing them to react with the sample introduced at varied concentrations. The count rates of H_3O^+, NO^+ and

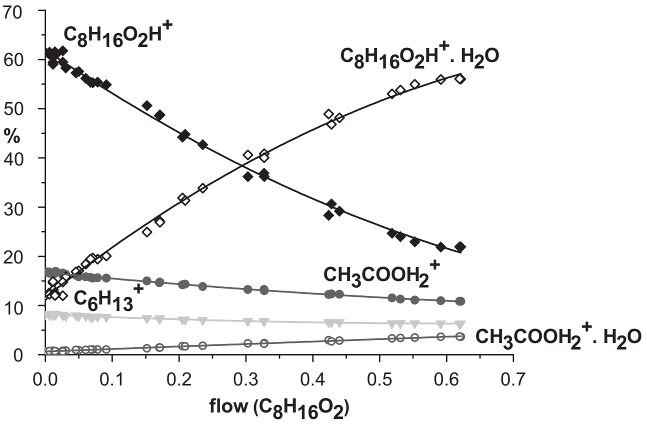

Fig. 1. A plot of percentages of individual product ions as a function of the flow rate of a mixture containing trace amount of hexyl acetate in humid air introduced into SIFT when H_3O^+ precursor ions are injected. The primary product branching ratios are obtained by extrapolating the lines to zero flow. Note that the sample flow rate is in relative units when flow = 1 corresponds to the e-fold reduction of the count rate of H_3O^+ due to the reaction with the studied compound.

$O_2^{+\bullet}$ were plotted on a semi-logarithmic scale as functions of the sample flow rate and the rate constants (k) for the NO^+ and $O_2^{+\bullet}$ reactions were determined from the relative slopes of these plots.

2.2. Kinetics of the ion chemistry involving water molecules: determination of three-body association rate constants

The reactions of most molecules M with H_3O^+ precursor ions generally result in the formation of nascent MH^+ ions. In the presence of water molecules, the H_3O^+ ions are partially converted to hydrated hydronium ions $H_3O^+(H_2O)_{1,2,3}$. These cluster ions can act as additional precursors and produce additional ion products like $MH^+(H_2O)_{1,2,3}$ via ligand switching reactions. The MH^+ product ions of proton transfer can also directly associate with H_2O similarly forming ions $MH^+(H_2O)_{1,2,3}$. Thus, the ion chemistry, which is important for real time and accurate quantification by SIFT-MS, is influenced by the presence of water vapour and it is necessary to account for this [27].

In SIFT-MS measurements using H_3O^+ precursor ions it is usually the case that both MH^+ and its hydrates $MH^+(H_2O)_{1,2,3}$ are formed. The ratio of the count rates of these ions change with the sample flow rate and the sample humidity and by recording these relative count rates the efficiency of clustering as a fundamental parameter, related to elementary rate constants, can be obtained. The objective of this section is to indicate the kinetic principles and the procedure adopted to analyse the experimental data.

Three-body rate constants for the association reactions of MH^+ ions with H_2O molecules in helium, k_{MH^+} describe the rate of hydration of the protonated molecules in the gas phase:

$$MH^+ + H_2O + He \rightarrow MH^+(H_2O) + He \tag{1}$$

In order to obtain these rate constants experimentally it is important to consider the role of $H_3O^+(H_2O)$ ions formed in the following three-body reaction described by the rate constant $k_{H_3O^+}$

$$H_3O^+ + H_2O + He \rightarrow H_3O^+(H_2O) + He \tag{2}$$

The three body-rate constant for reaction (2) has been previously determined to be $k_{H_3O^+} = 6 \times 10^{-28}\ \mathrm{cm^6\ s^{-1}}$ [27]. The cluster ions formed in reaction (2) contribute to the formation of $MH^+(H_2O)$ ions via ligand switching with M:

$$H_3O^+(H_2O) + M \rightarrow MH^+(H_2O) + H_2O \tag{3}$$

So these hydrated protonated molecules $MH^+(H_2O)$ can be produced by two parallel routes, viz reactions (1) and (3). The separate contribution of reaction (3) can be quantified by a parameter S_{eff} representing the contribution of the switching reactions to their formation taken relatively to the formation of hydrated hydronium ions [27]:

$$S_{eff} = \frac{\ln([MH^+] + [MH^+(H_2O)_{1,2,3}]_s/[MH^+])}{\ln([H_3O^+]_0/[H_3O^+])} \tag{4}$$

Here, $[MH^+]$ and $[H_3O^+]$ (or [19]) are the count rates of MH^+ and H_3O^+ ions detected by the downstream mass spectrometer, tacitly assumed to be proportional to the concentrations of the ions at the end of the flow tube. $[H_3O^+]_0$ is the count rate observed in the absence of water vapour, which is also equivalent to the sum of count rates of $H_3O^+(H_2O)_{0,1,2,3}$. The subscript s denotes the theoretical count rates of the $MH^+(H_2O)_{1,2,3}$ ions formed in switching reactions only, as calculated from the linearised kinetic equation (see [27]):

$$[MH^+(H_2O)_{1,2,3}]_s = [M]t\left([37]\frac{k_{37}}{2} + [55]\frac{k_{55}}{2} + [73]\frac{k_{73}}{2}\right) \tag{5}$$

where t is reaction time, k_{37}, k_{55} and k_{73} are the rate constants for the switching reactions of the respective hydrated hydronium ions with M and [37], [55], and [73] are the actual count rates of the $H_3O^+(H_2O)_{1,2,3}$ ions as observed in the experiments. The divisors 2 in Eq. (5) describe the fact that due to their continuous formation in the flow tube [27], reaction times of the $H_3O^+(H_2O)_{1,2,3}$ ions are approximately half the reaction time of H_3O^+. Thus:

$$S_{eff} = \frac{\ln(1 + ([M]t([37](k_{37}/2) + [55](k_{55}/2) + [73](k_{73}/2))/([M]t \cdot [19]k_{19})))}{\ln(1 + (([37] + [55] + [73])/[19]))} \tag{6}$$

By simplification of this expression the S_{eff} parameter can be calculated from the known rate constants and the experimental data as follows:

$$S_{eff} = \frac{\ln(1 + (([37](k_{37}/2) + [55](k_{55}/2) + [73](k_{73}/2))/([19]k_{19})))}{\ln(1 + (([37] + [55] + [73])/[19]))} \tag{7}$$

Similarly, the total contribution of both parallel routes of formation of the protonated hydrated ions, i.e., via the association reaction (1) and via the above switching reactions relative to that for the reaction of H_3O^+ with H_2O, can be described by a coefficient A_{eff}:

$$A_{eff} = \frac{2\ln(([MH^+] + [MH^+(H_2O)_{1,2,3}]_A)/([MH^+]))}{\ln([H_3O^+]_0/[H_3O^+])} \tag{8}$$

Again, the subscript 0 indicates the respective ion count rate in the absence of water vapour in the helium carrier gas. Thus, the $[MH^+]_0$ can be acquired during analysis as the sum of the $[MH^+]$ and $[MH^+(H_2O)_n]$ count rates (same as the procedure to determine $[H_3O^+]_0$). The factor 2 in Eq. (8) is again a compensation of the reaction time for continuously formed MH^+ ions, which is half of that for H_3O^+. Because A_{eff} is expressed in the terms of ion count rates only, it can be directly obtained from the experimental data such as mass spectra. An important test is that the experimental value of A_{eff} is invariant with [M] and also invariant with $[H_2O]$. The value of A_{eff} has a very simple interpretation as it describes how much faster clustering of MH^+ is compared to clustering of H_3O^+. Mathematically A_{eff} so defined and expressed by Eq. (8) agrees with A_{eff} as used in [27] however the verbal definition of A_{eff} in the previous paper [27] was not strictly speaking correct because it incorrectly neglected the contribution of switching.

Now the true contribution of association without switching is simply described as $A_{eff} - S_{eff}$ and the value of three-body association rate constant can be calculated as:

$$k_{MH^+} = (A_{eff} - S_{eff}) \cdot k_{H_3O^+}. \tag{9}$$

So k_{MH^+} obtained from Eq. (9) is a fundamental three body association rate constant anchored to the known value of $k_{H_3O^+}$. Numerical examples of calculations of A_{eff} and S_{eff} are given in Appendix A.

3. Results and discussion

3.1. Rate constants for the H_3O^+, NO^+ and $O_2^{+\bullet}$ reactions

The calculated rate constants, k_c, for the reactions of H_3O^+ with the esters and the experimentally determined rate constants, k, for the NO^+ and $O_2^{+\bullet}$ are summarized in Table 1. As can be seen, all experimental rate constants are within the experimental uncertainty ±20% equivalent to the theoretical collisional k_c values. The only exceptions are benzyl acetate where the NO^+ reaction proceeds only at 60% of k_c and methyl benzoate for which $O_2^{+\bullet}$ reaction apparently proceeds faster than k_c. A possible explanation for this is that the H_3O^+ rate constant is slower than k_c by about 20% or that the Su and Chesnavich theory is not precise for interactions of ions with geometrically large molecules. Unfortunately the current experimental method does not allow absolute determinations of the concentrations of volatile compounds such as methyl benzoate to accuracy better than 20%.

Table 1
Rate constants for the reactions of H_3O^+, NO^+ and $O_2^{+\bullet}$ with the six esters indicated, given in the units of 10^{-9} cm^3 s^{-1}. Also given are the molecular weights (MW), polarisabilities, α, and the dipole moments, μ_r, of these esters.

	Molecule	MW	α (10^{-24} cm^3)[a]	μ_r (D)[a]	H_3O^+ [k_c]	NO^+ k [k_c]	$O_2^{+\bullet}$ k [k_c]
Hexyl acetate	$C_8H_{16}O_2$	144	16.20	1.86	[3.2]	2.6 [2.6]	2.3 [2.6]
Benzyl acetate	$C_9H_{10}O_2$	150	16.90	2.00	[3.4]	1.9 [2.8]	2.5 [2.7]
Phenethyl acetate	$C_{10}H_{12}O_2$	164	18.56	2.04	[3.5]	2.9 [2.8]	3.0 [2.8]
Methyl salicylate	$C_8H_8O_3$	152	15.82	2.53	[3.8]	3.2 [3.1]	3.5 [3.0]
Methyl benzoate	$C_8H_8O_2$	136	15.07	2.01	[3.3]	2.4 [2.7]	3.5 [2.7]
Benzyl benzoate	$C_{14}H_{12}O_2$	212	24.78	2.08	[3.7]	2.5 [3.1]	2.8 [3.0]

[a] Values of α and μ_r are taken from the literature [22–25].

3.2. Ion products of the H_3O^+ reactions

The reactions of five of the six esters with H_3O^+ proceed via the formation of a protonated molecule, MH^+, which is the only ion product for the methyl salicylate reaction (in agreement with the previous study [8]) and the major ion product for the hexyl acetate and methyl benzoate. Benzyl benzoate reaction is an exception to this rule as it results only in formation of fragment product ions.

Partial fragmentation of the nascent MH^+ ions occurs in the hexyl acetate reaction leading to the formation of $C_2H_5O_2^+$ (m/z 61) and $C_6H_{13}^+$ (m/z 85):

$$\begin{array}{llll} H_3O^+ + C_8H_{16}O_2 & \rightarrow \quad C_8H_{16}O_2H^+ + H_2O & 77\% & (a) \\ & \rightarrow \quad C_2H_5O_2^+ + C_6H_{12} + H_2O & 16\% & (b) \\ & \rightarrow \quad C_6H_{13}^+ + C_2H_4O_2 + H_2O & 7\% & (c) \end{array} \qquad (10)$$

Note the likely release of a hexene molecule in reaction (10b) and an acetic acid molecule in reaction (10c).

The major product ion of benzyl acetate is $C_7H_7^+$ (m/z 91):

$$\begin{array}{llll} H_3O^+ + C_9H_{10}O_2 & \rightarrow \quad C_7H_7^+ + CH_3COOH + H_2O & 86\% & (a) \\ & \rightarrow \quad C_9H_{10}O_2H^+ + H_2O & 14\% & (b) \end{array} \qquad (11)$$

The $C_7H_7^+$ fragment is usually observed for electron ionisation (EI) mass spectra of aromatic compounds and is called the tropylium ion [28]. It is a heptagonal and planar, cyclic ion with 6 π-electrons. Note the parallel release of an acetic acid molecule. The minority product (11b) is the protonated parent molecule MH^+.

The tropylium ion is also formed in the benzyl benzoate reaction. Note that MH^+ is not produced at observable intensity in this reaction, which leads to two ion products with m/z identical to the products of the benzyl acetate reaction (m/z 151 and m/z 91). However the most plausible structure of the m/z 151 ion is $C_8H_7O_3^+$ implying that the water molecule from H_3O^+ is incorporated into the ion product:

$$\begin{array}{llll} H_3O^+ + C_{14}H_{12}O_2 & \rightarrow \quad C_8H_7O_3^+ + (C_6H_6 + H_2) & 60\% & (a) \\ & \rightarrow \quad C_7H_7^+ + C_7H_6O_2 + H_2O & 40\% & (b) \end{array} \qquad (12)$$

Note that formation of $C_9H_{11}O_2^+$ ion after proton transfer would require a very unlikely neutral product C_5H_2.

The H_3O^+ reaction with phenethyl acetate produces the $C_8H_9^+$ ion (80%) and, again, an acetic acid molecule and the protonated molecular ion $C_{10}H_{12}O_2H^+$ (20%).

The rate constants of the three-body association reactions of the MH^+ ions with water molecules (1), as determined according Section 2.2 (see also examples in Appendix A) are given in Table 2. The three protonated acetates form water clusters very efficiently (A_{eff} 6.6–21; note that A_{eff} for protonated acetone is 3.1), the k_{MH^+} being fastest for hexyl acetate, presumably because of the aliphatic chain has many vibrational degrees of freedom. Protonated methyl benzoate and the m/z product of the benzyl benzoate reaction ($C_8H_7O_3^+$) associate relatively slowly (A_{eff} 2.2 to 2.6) even though the proton affinity of methyl benzoate is very similar to that of hexyl acetate and thus any difference cannot be simply related to the energetics of a proton bound structures. A possible explanation why association of the protonated benzoates is slower than association of protonated acetates can be that it is due to steric hindrance when the charge is located in the inner parts of the ion and not on an accessible functional group, but this would have to be substantiated by quantum chemical modelling. Protonated methyl salicylate represents a very unusual exception in that, according to the value of k_{MH^+}, this ion does not associate with H_2O (see also the mass spectrum in Fig. 2 demonstrating the absence of an association product). Note that the PA of methyl salicylate is somewhat greater than that of the other esters; however, the difference is only 5–10 kJ/mol, but still much greater than the PA of H_2O at 690 kJ/mol. Again, we can only hypothesise that the reason for this observed anomaly is steric hindrance and that the charge is not located on an accessible functional group.

3.3. Ion products of the NO^+ reactions

The reactions of NO^+ with the esters proceed via three-body association reactions forming $M{\cdot}NO^+$ adduct ions or via charge transfer that in some cases results in fragmentation products [18]. The reaction with methyl salicylate proceeds as simple non-dissociative charge transfer in agreement with the previous study [8]. The benzyl benzoate reaction leads to several fragment ions including the tropylium ion. The reaction of NO^+ with hexyl acetate is an example of straightforward simple three-body association:

$$NO^+ + C_8H_{16}O_2 + He \rightarrow C_8H_{16}O_2{\cdot}NO^+ + He \qquad 100\% \qquad (13)$$

Table 2
Kinetic data for the formation of hydrates of the protonated esters indicated, as formed by ligand switching and three-body association.

Compound	P.A. (kJ/mol)[a]	S_{eff}[b]	A_{eff}[c]	k_{MH^+} (10^{-27} cm^6 s^{-1})[d]
Hexyl acetate	845	0.4	21.0	12.4
Benzyl acetate	n.a	0.4	10.7	6.2
Phenethyl acetate	n.a.	0.4	6.6	3.7
Methyl salicylate	855	0.4	0.3	<0.1
Methyl benzoate	850	0.4	2.6	1.3
$C_8H_7O_3^+$[e]	n.a.	0.4	2.2	1.1

[a] Proton affinities as taken from [7] are given where available; n.a. means that the P.A. is not known.
[b] Ligand switching efficiencies calculated from Eq. (7).
[c] Association efficiencies obtained from experimental data using Eq. (8).
[d] Three body association rate constants calculated from Eq. (9).
[e] Protonated benzyl benzoate was not observed, reported values refer to the fragment ion indicated.

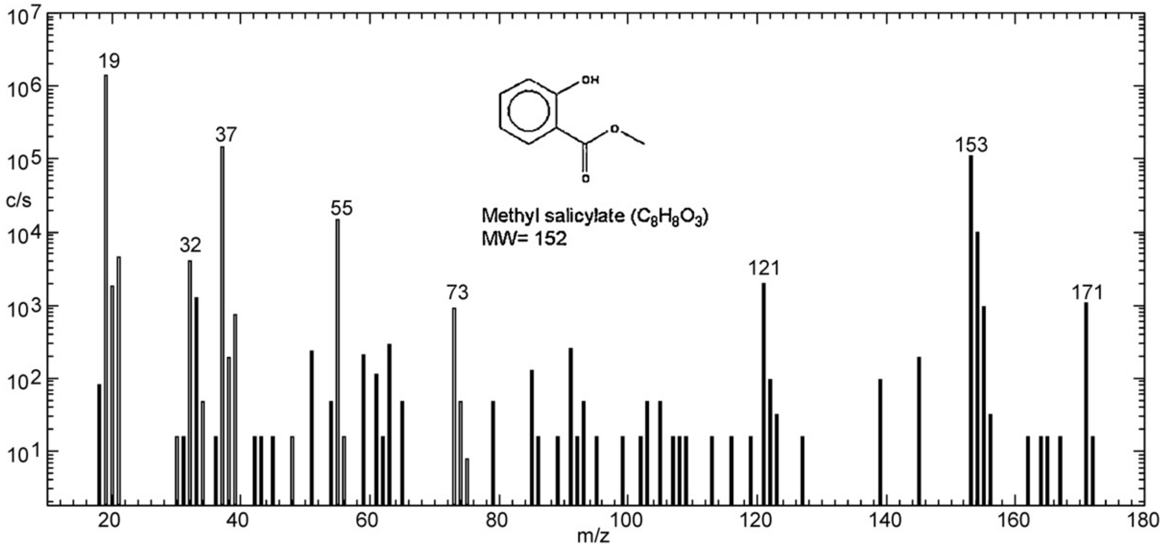

Fig. 2. The SIFT-MS spectrum obtained using the H_3O^+ precursor ions when methyl salicylate is introduced into the helium carrier gas; ion count rates are given on semi-logarithmic scale as a function of *m*/*z*. Note the characteristic ion products at *m*/*z* 121, 153 and the relatively small peak of the hydrated protonated parent molecule at *m*/*z* 171 that originates entirely from ligand switching reactions involving the hydrated hydronium ions at *m*/*z* 37, 55 and 73.

The benzyl acetate reaction:

$$\begin{array}{llcll} NO^+ + C_9H_{10}O_2 & \xrightarrow{He} & C_9H_{10}O_2 \cdot NO^+ & 27\% & (a) \\ & \rightarrow & C_9H_{10}O_2^{+\bullet} + NO^\bullet & 66\% & (b) \\ & \rightarrow & C_7H_8O^{+\bullet} + (C_2H_2O + NO^\bullet) & 7\% & (c) \end{array} \quad (14)$$

is an example of the three-body association reaction occurring in parallel with charge transfer producing the parent radical cation $M^{+\bullet}$. Unfortunately no values of ionisation potentials are available in the current literature for any of the six esters. However, on the basis of the present data we can conclude, that the ionisation potentials of benzyl acetate and methyl salicylate are less than ionisation potential of NO, 9.25 eV, because otherwise charge transfer would be endothermic and could not occur at room temperature.

The minor channel (14c) can be seen as a dissociative charge transfer or as a transfer of $C_2H_2O^-$ ion forming a neutral product $C_2H_2ONO^\bullet$.

3.4. Ion products of the $O_2{}^{+\bullet}$ reactions

Reactions with the $O_2{}^{+\bullet}$ precursor ion mostly proceed either via non-dissociative charge transfer producing the parent radical cation $M^{+\bullet}$ or via dissociative charge transfer reactions resulting in several fragment ions [18]. The methyl salicylate reactions exemplifies both of these processes:

$$\begin{array}{llcll} O_2^{+\bullet} + C_8H_8O_3 & \rightarrow & C_8H_8O_3{}^{+\bullet} + O_2 & 57\% & (a) \\ & \rightarrow & C_7H_6O_3^{+\bullet} + CH_2 + O_2 & 38\% & (b) \\ & \rightarrow & C_7H_4O_2^{+\bullet} + CH_3OH + O_2 & 5\% & (c) \end{array} \quad (15)$$

Note that our experimental data indicate that two fragment ions are produced (15b) and (15c) in addition to non-dissociative charge transfer that was previously reported by Iachetta et al. [8] to be the only reaction channel. It is worthy of note that all products of the $O_2{}^{+\bullet}$ reactions given in Table 3 are also present on the EI spectra [7] with the exception of benzyl benzoate, which on reaction with $O_2{}^{+\bullet}$ forms fragments that are not seen on EI spectra.

3.5. Avoiding m/z overlaps and optimised kinetic library entries for SIFT-MS

The SIFT-MS method of determination of absolute concentrations in real time is based on obtaining the ratio of the sum of several product ion count rates to the sum of the precursor ion count rates weighted by their reaction rate constants. Additional coefficients can be also applied to account for special circumstances such as overlaps of contributions from different characteristic ions at the same *m*/*z* value [29]. In analysis, these calculations are carried out by the SIFT-MS analytic software on-line taking the rate constants and other coefficients from the kinetic library [29]. Our objective was to construct entries for this kinetics library (i.e., define the sets of *m*/*z* values of product ions needed for quantification of the six esters together with the appropriate rate constants and with coefficients to be applied in order to minimise cross sensitivity between different compounds. These library entries will thus allow selective measurement of the concentrations of these six esters.

In the course of this work we initially simply chose to sum the count rates of all product ions of the H_3O^+ reactions given in Table 3 together with their hydrates. This was done by listing the product ions in the kinetic library with all f_p coefficients (used to multiply the corresponding ion count rates) set as 1.0. Validations of this initial kinetic library using reference mixtures of the six esters in air at approximately 10 ppm concentrations indicated *m*/*z* overlaps between hexyl acetate and phenethyl acetate and then amongst the group of benzoates (see Fig. 3a). Only methyl salicylate was quantified without any signs of overlap. The *m*/*z* overlaps between hexyl acetate and phenethyl acetate was caused due to the *m*/*z* 61 and 79 ions. The product branching ratios of *m*/*z* 61 and its hydrate 79 was less than 5% for phenethyl acetate (and this it does not even appear in Table 3) and 16% for hexyl acetate (see Table 3). To avoid this overlap problem we have excluded these *m*/*z* values from the final kinetic library entry (given in Table 4) for phenethyl acetate. Other overlaps amongst benzoates were caused by the same *m*/*z* values of the ion products of the benzyl acetate and benzyl benzoate reactions (91, 151, and 169). The methyl benzoate reaction leads to a small *m*/*z* 91 product (less than 2%) and thus we excluded this product ion from the methyl benzoate entry.

Somewhat more challenging was to resolve the *m*/*z* overlaps between benzyl acetate and benzyl benzoate. The three main ion products (including one hydrate) of the reactions of these two esters are the same (*m*/*z* 91, 151 and 169); however the percentages of product branching ratios are significantly different (Table 3). Thus, we have exploited this difference in order to distinguish these

Table 3
The product ions and the corresponding branching ratios for the reactions of H_3O^+, NO^+ and $O_2^{+\bullet}$ with the six esters in helium carrier gas at 300 K.

Compound	MW	Formula	H_3O^+	m/z[a]		NO^+	m/z	$O_2^{+\bullet}$	m/z[a]	
Hexyl acetate	144	$C_8H_{16}O_2$	77% $C_8H_{16}O_2H^+$	145	(163)	100% $C_8H_{16}O_2NO^+$	174	73% $C_6H_{12}^{+\bullet}$	84	
			16% $CH_3COOH_2^+$	61	(79)			27% $C_2H_5O_2^+$	61	(79)
			7% $C_6H_{13}^+$	85						
Benzyl acetate	150	$C_9H_{10}O_2$	86% $C_7H_7^+$	91		66% $C_9H_{10}O_2^{+\bullet}$	150	88% $C_7H_8O^{+\bullet}$	108	(126)
			14% $C_9H_{10}O_2H^+$	151	(169)	27% $C_9H_{10}O_2NO^+$	180	12% $C_9H_{10}O_2^{+\bullet}$	150	
						7% $C_7H_8O^{+\bullet}$	108			
Phenethyl acetate	164	$C_{10}H_{12}O_2$	80% $C_8H_9^+$	105		84% $C_8H_8^{+\bullet}$	104	100% $C_8H_8^{+\bullet}$	104	
			20% $C_{10}H_{12}O_2H^+$	165	(183)	16% $C_{10}H_{12}O_2NO^+$	194			
Methyl salicylate	152	$C_8H_8O_3$	100% $C_8H_8O_3H^+$	153	(171)	100% $C_8H_8O_3^{+\bullet}$	152	57% $C_8H_8O_3^{+\bullet}$	152	
								38% $C_7H_6O_3^{+\bullet}$	138	
								5% $C_7H_4O_2^{+\bullet}$	120	
Methyl benzoate	136	$C_8H_8O_2$	93% $C_8H_8O_2H^+$	137	(155)	41% $C_8H_9^+$	105	62% $C_8H_8O_2^{+\bullet}$	136	
			7% $C_8H_9^+$	105		53% $C_8H_8O_2NO^+$	166	38% $C_7H_5O^+$	105	
						6% $C_8H_8O_2^{+\bullet}$	136			
Benzyl benzoate	212	$C_{14}H_{12}O_2$	60% $C_8H_7O_3^+$	151	(169)	45% $C_9H_{10}O_2NO^+$	180	46% $C_7H_8O^{+\bullet}$	108	
			40% $C_7H_7^+$	91		25% $C_7H_7O^+$	107	23% $C_7H_6O_2^{+\bullet}$	122	
						18% $C_7H_5O^+$	105	10% $C_9H_{10}O_2^{+\bullet}$	150	
						12% $C_7H_7^+$	91	16% $C_6H_7^+$	79	

[a] m/z of the primary products with branching ratios >5% only are given (m/z of hydrated product ions are given in parentheses).

two compounds. The main idea in constructing the final kinetic library entries for these compounds is to find linear combinations of ion product count rates that would allow selective quantification of different compounds. Note that for this purpose the ion count rates of hydrated ions (when these are formed) should be added to the ion count rates of the corresponding primary product ions in order to ensure that the results will be valid for any concentration of H_2O in sample. Such linear combination can be found by the

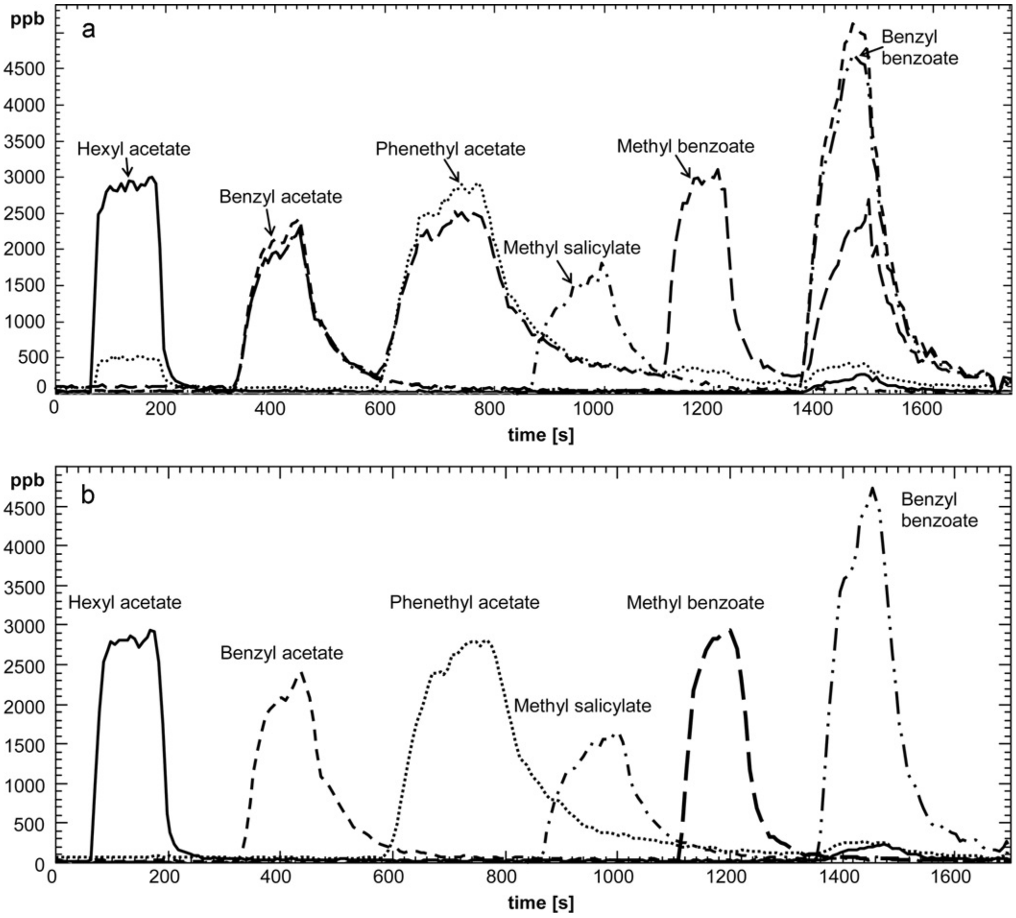

Fig. 3. (a) Time profile of the concentration of the six esters calculated (in ppb) simply from the sum of the characteristic product ions in a validation experiment when diluted samples of reference compounds are introduced sequentially. Note that overlaps between m/z values of products cause cross-sensitivity between hexyl acetate and phenethyl acetate and amongst the group of benzoates. (b) The same raw experimental data evaluated using the optimised kinetic library as given in Table 4; note that cross sensitivity has been dramatically reduced.

Table 4
SIFT-MS kinetics library in the format required by the SIFT-MS software for on-line calculations of the concentrations of the six esters, optimised for minimum cross sensitivity (see the text for further discussion).

Hexyl acetate (H_3O^+)			Phenethyl acetate (H_3O^+)			Methyl salicylate (H_3O^+)			Methyl benzoate (H_3O^+)			Benzyl benzoate (H_3O^+)		
4 Precursors			4 Precursors			4 Precursors			4 Precursors			4 Precursors		
19	3.2e−9	1.0	19	3.5e−9	1.0	19	3.8e−9	1.0	19	3.3e−9	1.0	19	3.7e−9	1.0
37	2.4e−9	1.0	37	2.6e−9	1.0	37	2.9e−9	1.0	37	2.5e−9	1.0	37	2.8e−9	1.0
55	2.1e−9	1.0	55	2.2e−9	1.0	55	2.5e−9	1.0	55	2.2e−9	1.0	55	2.4e−9	1.0
73	1.9e−9	1.0	73	2.0e−9	1.0	73	2.2e−9	1.0	73	2.0e−9	1.0	73	2.1e−9	1.0

Hexyl acetate (H_3O^+)		Benzyl acetate (H_3O^+)		Phenethyl acetate (H_3O^+)		Methyl salicylate (H_3O^+)		Methyl benzoate (H_3O^+)		Benzyl benzoate (H_3O^+)	
5 Products		3 Products		6 Products		3 Products		3 Products		3 Products	
61	1.0	91	1.38	105	1.088	121	1.077	137	1.236	91	−0.30
79	1.0	151	−0.86	137	−0.06	153	1.088	155	1.088	151	1.96
85	1.066	169	−0.86	155	−0.06	171	1.088	153	−0.16	169	1.96
145	1.088			163	−0.01						
163	1.088			165	1.1						
				183	1.1						

simple solution of a set of the linear equations:

$$\begin{aligned} A &= f_A\,[91]_A + g_A\,[151+169]_A \quad \text{(a)} \\ B &= f_B\,[91]_B + g_B\,[151+169]_B \quad \text{(b)} \end{aligned} \tag{16}$$

Here A represents the linear combination used to quantify benzyl acetate and B represents the linear combination to quantify benzyl benzoate. The square brackets indicate the product ion count rates registered when the compound indicated by subscripts A (benzyl acetate) and B (benzyl benzoate) is introduced into SIFT-MS. The constraints on the coefficients *f* and *g* (treated as the unknowns in the set of equations) are given by the requirement of calculating zero concentration of A when only B is introduced and vice versa:

$$\begin{aligned} 0 &= f_A\,[91]_B + g_A\,[151+169]_B \quad \text{(a)} \\ 0 &= f_B\,[91]_A + g_B\,[151+169]_A \quad \text{(b)} \end{aligned} \tag{17}$$

Now it is possible to calculate *f* and *g* coefficients from the experimental data of ion count rates using the pure compounds. For the case of benzyl acetate and benzyl benzoate the results are: $f_A = 1.38$, $g_A = -0.86$, $f_B = -0.30$ and $g_B = 1.96$. Details of calculation for these two compounds are given in Appendix B. Similar experiments and calculations were used to resolve other *m*/*z* overlaps. The final kinetics library entries as given in Table 4 were then used to calculate concentrations of all these six esters in the H_3O^+ validation experiment and, as can bee seen in Fig. 3b, cross sensitivity has been successfully minimised using this kinetic library. Finally, it is worthy of a note that the *m*/*z* 91 product of benzyl acetate overlaps with the $H_3O^+(H_2O)_4$ water cluster and thus NO^+ that leads to *m*/*z* 150 and 180 characteristic product ions is a more suitable precursor ion for this compound, however *m*/*z* 180 is a main product of benzyl benzoate and thus only *m*/*z* 150 should be used with an appropriate coefficient.

4. Concluding remarks

The data obtained in this study allow SIFT-MS analyses of phytogenic esters in the presence of water vapour. On the basis of these data it is now possible to use SIFT-MS to study ester emissions from plants and possibly also from other organisms such as bacteria. The combination of the three different precursor ions used for SIFT-MS provides a tool to diminish ambiguity and to positive identify the esters in mixtures of volatile compounds in air. Protonated esters have a propensity to form cluster ions with water molecules and the rate constants for such reactions have been also obtained in this study. As a practical outcome, in addition to fundamental ion kinetics data, SIFT-MS kinetic library entries have been constructed that allow selective quantification of these esters in spite of some overlaps between the *m*/*z* values of characteristic product ions.

Acknowledgements

We thank Violetta Shestivska for introducing us to the field of phytoremediation and her help with some of the present experiments, to Ondřej Zemek for providing reference samples of the esters and to David Smith for his careful reading and editing of the manuscript. We gratefully acknowledge financial support by the Grant Agency of the Czech Republic (projects number 202/09/0800 and 203/09/0256) and by Grant Agency of Charles University (project GAUK 32010).

Appendix A. Numerical examples of the calculations of the parameters S_{eff}, A_{eff} and k_{MH^+} for hexyl acetate and methyl salicylate

The experimental precursor and product ion count rates (corrected for mass discrimination and differential diffusion) for H_3O^+ reactions of hexyl acetate and methyl salicylate are given in Table A.1. The data were acquired in the MIM mode, as described in Section 2.1. The symbols k_{19}, k_{37}, k_{55} and k_{73} indicate the rate constants for the proton transfer reaction and for the switching reactions of the respective hydrated hydronium ions with M and are calculated according Su and Chesnavich [21]. Square brackets [19], [37], [55], and [73] indicate the actual count rates of the $H_3O^+(H_2O)_{1,2,3}$ ions and $[MH^+]$ and $[MH^+(H_2O)]$ are the actual count rates of the protonated molecule of a sample and its hydrate.

Assigning these numerical values for hexyl acetate to Eq. (7) gives the value $S_{eff} = 0.4$. Using the values from Table A.1 in Eq. (8) gives.

$$A_{eff} = \frac{2\ln((([198802+337378]_0)/[198802]))}{\ln(([1108200+96514+12455+1018]_0)/[1108200])} = 21.0 \tag{A.1}$$

Finally combining these two numbers with the known rate constant gives $k_{MH^+} = (21.0 - 0.4) \cdot 6.0 \cdot 10^{-28} = 12.4 \cdot 10^{-27}\ \mathrm{cm^6\,s^{-1}}$.

Analogical calculation for methyl salicylate provides according to Eq. (7) the same result for $S_{eff} = 0.4$ however the value of A_{eff} according to Eq. (8) is much smaller:

$$A_{eff} = \frac{2\ln(([135510+2029]_0)/[135510])}{\ln(([1856555+177350+14608+703]_0/[1856555]))} = 0.3 \tag{A.2}$$

The fact that A_{eff} is very close to S_{eff} (actually somewhat smaller in this example) means that within the experimental error association does not measurably contribute to the formation of the hydrated protonated ions.

Table A.1
Experimental count rates and rate constants used in this example.

M	c/s				k (10^{-9} cm^3 s^{-1})					c/s[MH$^+$(H$_2$O)]
	[19]	[37]	[55]	[73]	k_{19}	k_{37}	k_{55}	k_{73}	[MH$^+$]	
Hexyl acetate	1108200	96514	12455	1018	3.2	2.4	2.1	1.9	198802	337379
Methyl salicylate	1856555	177350	14608	733	3.8	2.9	2.5	2.2	135510	2029

Appendix B. Numerical examples illustrating optimisation of the kinetic library entries for minimisation of the effect of overlaps.

This appendix illustrate the numerical calculations used in obtaining the f_p coefficients for benzyl acetate and benzyl benzoate accounting for the overlaps of the ion products at m/z 91, 151 and 169 according to the procedure explained in Section 3.5. The experimental count rates (in c/s after correction for mass discrimination and differential diffusion) were obtained when benzyl acetate (symbol A) was introduced as $[91]_A = 8606$, $[151]_A = 609$, $[169]_A = 746$ and when benzyl benzoate (symbol B) was introduced as $[91]_B = 8822$, $[151]_B = 11088$, $[169]_B = 3318$.

The solution to a set of linear equations (17a) and (17b) for these count rates is

$$f_A = -g_A \frac{[151+169]_B}{[91]_B} = -g_A \cdot 1.63 \tag{B.1}$$

$$f_B = -g_B \frac{[151+169]_A}{[91]_A} = -g_B \cdot 0.157 \tag{B.2}$$

The coefficients g_A, g_B, f_A and f_B can now be calculated by solving the following set of equations obtained from (16a) and (16b):

$$9961 = -g_A \cdot 12698 \tag{B.3}$$

$$23228 = -g_B \cdot 13017 \tag{B.4}$$

as $f_A = 1.28$, $g_A = -0.78$, $f_B = -0.28$, $g_B = 1.78$.

Finally in order to produce practically applicable accurate kinetics library it is important to account for the isotopic abundance of ^{13}C by multiplying these coefficient by 1.077 for m/z 91 and 1.099 for m/z 151 and 169.

References

[1] J. Peñuelas, J. Llusià, Biologia Plantarum 41 (1998) 139–143.
[2] R. Fall, A.A. Benson, Trends in Plant Science 1 (1996) 296–301.
[3] G. König, M. Brunda, Atmospheric Environment 29 (1995) 861–874.
[4] R. Fall, T. Karl, A. Hansel, A. Jordan, W. Lindinger, Journal of Geophysical Research-Atmospheres 104 (1999) 15963–15974.
[5] M.R. Kant, P.M. Bleeker, M. Van Wijk, R.C. Schuurink, M.A. Haring, Plant volatiles in defence, in: Plant Innate Immunity, 2009, pp. 613–666.
[6] J.G. De Boer, M.A. Posthumus, M. Dicke, Journal of Chemical Ecology 30 (2004) 2215–2230.
[7] P.J. Linstrom, W.G. Mallard, NIST Chemistry WebBook, NIST Standard Reference Database Number 69, National Institute of Standards and Technology, Gaithersburg, 2010.
[8] L. Iachetta, L. Malek, B.M. Ross, Rapid Communications in Mass Spectrometry 24 (2010) 815–822.
[9] P. Španěl, D. Smith, International Journal of Mass Spectrometry 172 (1998) 137–147.
[10] N. Schoon, C. Amelynck, L. Vereecken, E. Arijs, International Journal of Mass Spectrometry 229 (2003) 231–240.
[11] T.S. Wang, P. Španěl, D. Smith, International Journal of Mass Spectrometry 228 (2003) 117–126.
[12] U.S.R. Rose, A. Manukian, R.R. Heath, J.H. Tumlinson, Plant Physiology 111 (1996) 487–495.
[13] L. Tollsten, P.M. Muller, Phytochemistry 43 (1996) 759–762.
[14] W. Lindinger, A. Hansel, A. Jordan, Chemical Society Reviews 27 (1998) 347–354.
[15] E. Aprea, F. Biasioli, T.D. Mark, F. Gasperi, International Journal of Mass Spectrometry 262 (2007) 114–121.
[16] M. Demarcke, C. Amelynck, N. Schoon, F. Dhooghe, H. Van Langenhove, J. Dewulf, International Journal of Mass Spectrometry 279 (2009) 156–162.
[17] E. Joo, J. Dewulf, M. Demarcke, C. Amelynck, N. Schoon, J.F. Muller, M. Simpraga, K. Steppe, H. Van Langenhove, International Journal of Mass Spectrometry 291 (2010) 90–95.
[18] D. Smith, P. Španěl, Mass Spectrometry Reviews 24 (2005) 661–700.
[19] K. Dryahina, M. Polášek, P. Španěl, International Journal of Mass Spectrometry 239 (2004) 57–65.
[20] G. Bouchoux, J.Y. Salpin, D. Leblanc, International Journal of Mass Spectrometry and Ion Processes 153 (1996) 37–48.
[21] T. Su, W.J. Chesnavich, Journal of Chemical Physics 76 (1982) 5183–5185.
[22] G.P. Johari, Digest of Literature on Dielectrics, National Academy of Sciences, Washington, DC, 1977.
[23] C.S. Copeland, M.W. Rigg, Journal of American Chemical Society 73 (1951) 5.
[24] http://www.thegoodscentscompany.com/, last accessed on October 2010.
[25] R. Weast, CRC Handbook of Chemistry & Physics. 66th ed., CRC, Boca Raton, FL, 1988.
[26] D. Smith, A. Pysanenko, P. Španěl, International Journal of Mass Spectrometry 281 (2009) 15–23.
[27] P. Španěl, D. Smith, Rapid Communications in Mass Spectrometry 14 (2000) 1898–1906.
[28] W.V. Doering, L.H. Knox, J. Am. Chem. Soc. 76 (1954) 3203–3206.
[29] P. Španěl, K. Dryahina, D. Smith, International Journal of Mass Spectrometry 249 (2006) 230–239.